

Metallicity effects on the cosmic SNIb/c and GRB rates

V. Grieco^{1*} F. Matteucci^{1,2} G. Meynet³ F. Longo¹ M. Della Valle⁴ R. Salvaterra⁵

¹*Dipartimento di Fisica, Sezione di Astronomia, Università di Trieste, via G.B. Tiepolo 11, I-34131, Trieste, Italy*

²*I.N.A.F. Osservatorio Astronomico di Trieste, via G.B. Tiepolo 11, I-34131, Trieste, Italy*

³*Observatory of the University of Geneva, CH1290 Versoix, Switzerland*

⁴*I.N.A.F. Osservatorio Astronomico di Capodimonte, Salita Moiariello, 16, 801313, Napoli, Italy*

⁵*I.N.A.F. IASF-Milano, via Bassini 15, I-20133, Milano, Italy*

Accepted . . ; in original form 2011

ABSTRACT

Supernovae Ib/c are likely to be associated to long GRBs, therefore it is important to compare the SN rate in galaxies with the GRB rate. To do that we computed Type Ib/c SN rates in galaxies of different morphological type (ellipticals, spirals and irregulars) by assuming different histories of star formation and different supernova Ib/c progenitors. We included some recent suggestions about the dependence of the minimum mass of single Wolf-Rayet (WR) stars upon the stellar metallicity and therefore upon galactic chemical evolution. We adopted several cosmic star formation rates (i.e. relative to a comoving unitary volume of the Universe) as functions of cosmic time, either observationally or theoretically derived, including the one computed with our galaxy models. Then we computed the cosmic Type Ib/c SN rates. Our results show that the predicted Type Ib/c SN rates in spirals and irregulars can well reproduce the present time observed rates if both single WR stars and massive binary systems are taken into account as Type Ib/c SN progenitors. The metallicity effects on the minimum mass for single WR stars are evident mainly in the early phases of galaxy evolution and do not influence substantially the predicted local Type Ib/c rates. We derived the following conclusions: i) the ratio cosmic GRB - Type Ib/c rate varies in the range $10^{-2} - 10^{-4}$ in the whole redshift range, thus suggesting that only a small fraction of all the Type Ib/c SNe gives rise to GRBs. ii) The metallicity dependence of Type Ib/c SN progenitors produces lower cosmic SN Ib/c rates at early times, for any chosen cosmic star formation rate. iii) Different theoretical cosmic star formation rates, computed under different scenarios of galaxy formation, produce SN Ib/c cosmic rates which differ mainly at very high redshift. However, it is difficult to draw firm conclusions on the high redshift trend because of the large uncertainties in the data. iv) GRBs can be important tracers of star formation at high redshift if their luminosity function does not vary with redshift and they can help in discriminating among different galaxy formation models.

Key words: supernovae – gamma-ray bursts – galaxy evolution.

1 INTRODUCTION

Gamma Ray Bursts (GRB) are sudden and powerful gamma-ray flashes, occurring at a rate of ~ 1 per day in the Universe. The duration of GRBs at MeV energies ranges from 10^{-3} sec to about 10^3 sec, with long bursts being characterized by a duration > 2 seconds. In the past years, it has been established that some long GRBs are associated to supernovae (SNe) originating from the death of massive stars. The GRBs have been associated with powerful supernovae Ib/c having energies in excess of the majority of

such SNe and for this reason they have been called “hypernovae” (Iwamoto et al. 1998; see also Paczyński 1998). In particular, most of the evidence points towards Type Ic SNe (see Woosley & Bloom 2006, Hjorth & Bloom 2011). The “collapsar” model proposed to explain long GRBs takes into account this phenomenological aspect and proposes a Wolf-Rayet progenitor which undergoes core collapse, thus producing a rapidly rotating black hole surrounded by an accretion disk which injects energy into the system and thus acts as a “central engine” (Woosley 1993, MacFayden & Woosley 1999, Zhang, Woosley & MacFayden 2003). However, the collapsar can originate also in massive stars in binary systems, as suggested by several authors (e.g. Baron,

* E-mail: grieco@oats.inaf.it

1992; Kobulnicky & Fryer, 2007; Yoon et al. 2010). Detailed galaxy evolution models are able to predict the temporal behaviour of SN rates in galaxies of all morphological types. Therefore, a comparison between theoretical SN Ib/c rates and observed GRB rates seems appropriate at the present time. Bissaldi et al. (2007) already attempted such a comparison but the data relative to GRBs were much less than at the present time and limited to lower redshifts. At the present time, GRBs have been observed up to $z \sim 8.2$ (Salvaterra et al. 2009; Tanvir et al. 2009). In this paper we aim at studying the behaviour of the SN Ib/c rate in galaxies and as a function of redshift and compare it with the most recently derived cosmic GRB rate. In computing the Type Ib/c SN rate in galaxies we will adopt both single Wolf-Rayet and massive binaries as GRB progenitors and we will consider a dependence of the SN Ib/c progenitors on the initial stellar metallicity, not considered in any previous similar work (e.g. Bissaldi et al. 2007). Our intention is to make predictions for the rates of Type Ib/c supernovae at various redshift in spiral and irregular galaxies. At the moment, no observations can constraint such predictions, but in the future new powerful observational devices as the James Webb telescope or ELT will provide extensive and constraining observational constraints on those rates. The comparisons with the present predictions will then allow to confirm or reject the present predictions and will bring new clues on the nature of the Type Ib/c supernovae progenitors and on the star formation histories in spiral and irregular galaxies. From the comparison between observed GRB cosmic rate and predicted cosmic SN Ib/c rate, we aim first to check whether the present ratio of GRB to that of SN Ib/c can be well reproduced by our models, second to see how this ratio may change with redshift in the frame of our model. In Section 2 we will describe the chemical evolution model adopted to compute the evolution of galaxies of different morphological type, as well as the computation of the SN Ib/c rate. In Section 3 the computed SN Ib/c rates for irregular and spiral galaxies of different masses are presented and compared to the observed rates. In section 4 we assemble different cosmic histories of star formation, including the one computed by means of our galaxy models, to compute the cosmic Type I b/c SN rate, then we compare this cosmic SN rate with the cosmic GRB rate. Finally, in Section 5 a discussion and some conclusions are presented.

2 THE CHEMICAL EVOLUTION MODELS

In order to compute the Type Ib/c SN rate in galaxies we need to know the galaxy star formation history. Galaxies of different morphological type (ellipticals, spirals, irregulars) are characterized by different star formation histories (see Matteucci 2001). In particular, ellipticals should have suffered an intense and short star formation episode, whereas spirals and irregulars should have had milder star formation rates (SFR) and are still forming stars now. Irregular galaxies must have suffered the mildest SFR since they contain more gas than galaxies of other types. Here, we focus on irregular and spiral galaxies for the following reasons: i) because the SNe Ib/c are observed only in star forming galaxies and ii) because the observations on the hosts of GRBs have revealed that long GRBs are associated with faint, blue and

often irregular galaxies (Conselice et al. 2005; Fruchter et al. 2006; Tanvir & Levan 2007; Wainwright et al. 2007; Li 2008) and tend to occur in galaxies with low metallicities (Fynbo & al. 2003, 2006a; Prochaska et al. 2004; Soderberg et al. 2004; Gorosabel et al. 2005; Berger et al. 2006; Savaglio 2006; Stanek et al. 2006; Wolf & Podsiadlowsky 2007; Modjaz et al. 2008; Savaglio et al. 2009).

However, we do not exclude that this could be a selection effect (see e.g. Mannucci et al. 2011; Campisi et al. 2011). In particular, in the paper of Mannucci et al. (2011), the authors suggest that probably the region high- z /high mass is populated by the dark GRBs. This idea is partially confirmed by the observations of some dark GRB host galaxies provided by Kruhler et al. (2011), where the mass of the dark GRB hosts seem to be higher than the mass of the normal GRB hosts.

To do that we use a detailed self-consistent chemical evolution model reproducing the majority of the properties of irregular and spiral galaxies. The irregular galaxies play an important role in the study of chemical evolution and star formation owing to their simpler structure and lack of evolution compared to spiral galaxies. We also adopt a relatively simple model for spirals without taking into account gradients along the disk.

We assume that both irregular and spiral galaxies assemble all of their mass by means of a continuous infall of pristine gas. This is certainly true for spiral disks such as that of the Milky Way (see e.g. Chiappini et al. 1997; 2001; Boissier & Prantzos 1999). The basic equations are:

$$\dot{G}_i = -\psi(t)X_i(t) + R_i(t) + (\dot{G}_i)_{inf} - \dot{G}_{iw}(t) \quad (1)$$

where $G_i(t) = M_{gas}(t)X_i(t)/M_{inf}$ is the gas mass in the form of an element i normalized to the present time total luminous infall mass. The quantity $X_i(t) = G_i(t)/G(t)$ represents the abundance by mass of an element i and by definition the summation over all the elements present in the gas mixture is equal to unity. The quantity $G(t) = M_{gas}(t)/M_{inf}$ is the total fractional mass of gas. The quantity, $R_i(t)$ represents the rate at which the element i is restored into the ISM by the dying stars. Finally, $(\dot{G}_i)_{inf}$ and $\dot{G}_{iw}(t)$ represent the infall and wind rate, respectively.

The SFR ($\psi(t)$), namely the amount of interstellar gas, expressed in solar masses, turning into stars per unit time, is assumed to be continuous and defined as a Schmidt (1959) law:

$$\psi(t) = \nu G(t) \quad (2)$$

where the quantity ν is the star formation efficiency (SFE), namely the inverse of the typical time-scale for star formation, and is expressed in Gyr^{-1} . The SFE for spirals is assumed to be higher than in irregulars.

We explored one initial mass functions (IMF), in particular the Salpeter (1955) one ($x=1.35$ in the mass range $0.1-100 M_{\odot}$).

A main assumption of the model for irregulars is the existence of galactic winds triggered by SN explosions. In particular, it is assumed that a fraction ($\sim 30\%$) of the initial blast wave energy of SNe is transformed into thermal gas energy and the wind starts when the thermal energy of gas equates the binding energy of gas. The wind can be “normal”, namely each element is lost at the same rate, or “differential”, in the sense that some elements (metals for ex-

ample) are preferentially lost (see Bradamante et al. 1998). The galactic wind is likely to occur in these systems because of their relatively low potential well. Moreover, galactic outflows are observed in irregular galaxies (see e.g. Martin, 1999; Martin et al. 2002). To do that we follow the method described in Bradamante et al. (1998) and Yin et al. (2010); in particular, the wind rate is assumed to be proportional to the SFR through a free parameter λ_i larger than zero:

$$\dot{G}_{iw}(t) = \lambda_i \psi(t) \quad (3)$$

where i represents a specific chemical element. To have a preferential loss of metals, as indicated by dynamical models (e.g. Mc Low & Ferrara, 1999), we use a differential wind in which $\lambda_H = \lambda_{He} = 0.3$ and $\lambda_i \sim 0.9$ for the other elements.

In the case of spirals, the galactic wind is less likely to occur, owing the deep potential well in which the spiral disks lie. In fact, in spiral disks it is more likely to have galactic fountains rather than galactic winds (Spitoni et al. 2009).

Finally, the assumed rate of infall is the same for irregulars and spirals and follows the law:

$$(\dot{G}_i)_{inf} = \frac{a X_i e^{-t/\tau}}{M_{inf}}, \quad (4)$$

where a is a suitable constant, derived by integrating eq. (3) over the galactic lifetime, $(X_i)_{inf}$ is the abundance by mass of the element i in the infalling gas, assumed to be primordial and τ is the infall timescale. This timescale is expressed in Gyrs and defined as the characteristic time at which half of the total mass of the system has assembled. The values of τ are derived as the best ones in order to reproduce the majority of the observational constraints. This timescale is different for galaxies of different morphological type, being quite short in spheroids and increasing for spirals and irregulars.

In Table 1 we show the adopted model parameters for a typical spiral galaxy (Milky Way-like) and for a typical irregular galaxy. The infall mass M_{inf} is the mass that eventually would be accreted if no galactic wind would occur. Model Irr is described by an infall mass of $5 \cdot 10^9 M_\odot$ which is one order of magnitude lower than the infall mass of Model Sp. The infall timescale for the spiral galaxy is assumed to be 6 Gyr, although in the Milky Way disk the timescale for disk formation should have been shorter in the internal than in the external regions (inside-out formation, Matteucci & François 1989; Chiappini et al. 1997); here we want only to show some averaged properties and 6 Gyr is an average timescale between the internal timescales (~ 2 Gyr) and the external ones ($\sim 10 - 12$ Gyr). The timescale for the formation of irregulars is assumed to be smaller (4 Gyr). Always in Table 1 we report the wind parameter for irregular galaxies (λ_i , eq. 3) and the SFE for irregulars and spirals. By following the work of Calura et al. (2009) we assumed that the SFE increases with galactic mass.

Finally, in order to compute the cosmic star formation rate (CSFR) and Type Ib/c SN rate we have also considered a model for a typical elliptical of 10^{11} luminous mass. This model predicts a short and intense burst of star formation which stops before 1 Gyr, owing to the occurrence of strong galactic winds which devoid the galaxy of gas. The SFE adopted for this elliptical is 10 Gyr^{-1} implying that this galaxy assembles more quickly than the late type ones. The assumed IMF is the Salpeter one, as assumed also for

	Model Irr	Model Sp
$M_{inf} [M_\odot]$	$5 \cdot 10^9$	$5 \cdot 10^{10}$
$\tau [\text{Gyr}]$	3	6
λ_i	differential	no wind
$SFE [\text{Gyr}^{-1}]$	0.05	2

Table 1. Parameter sets used for describing our models: M_{inf} is the final total assembled mass if nothing is lost, τ is the infall time scale, λ_i is the wind parameter (see eq. 3) and SFE is the star formation efficiency.

the other galaxy types. It is worth noting that this model, such as the others for spirals and irregulars, well reproduce the local properties of ellipticals (Calura & Matteucci 2004; Pipino & Matteucci 2004). The star formation history of this elliptical is shown in Figure 1 together with the SFRs of a spiral and an irregular galaxy.

2.0.1 Nucleosynthesis and stellar evolution prescriptions

Since we computed the chemical evolution of these galaxies, in particular the evolution of the O abundance, we adopted the yields from massive stars by Woosley & Weaver (1995), the yields from low and intermediate mass stars by van den Hoek & Groenewegen (1997) and the yields from Type Ia SNe by Iwamoto et al. (1999), their model W7. Concerning the progenitors of Type Ib/c SNe it has been suggested that they could be single Wolf-Rayet (WR) stars, namely stars which have lost most of their H and He envelope and with masses larger than M_{WR} , whose value depends on the initial stellar metallicity. In fact, the mass loss in massive stars ($M \geq 10 M_\odot$) increases with the initial metallicity in a way that M_{WR} decreases with increasing metallicity (see Tables 2,3). In other words, with a high rate of mass loss, even stars of $20-25 M_\odot$ can become WRs. However, the progenitors of Type Ib/c SNe could also be massive stars in binary systems in the mass range $12-20 M_\odot$ (e.g. Baron, 1992; Bissaldi et al. 2007) or $14.8-45 M_\odot$ (Yoon et al. 2010). Here we consider both progenitors (see Smartt 2009) following in part the work of Bissaldi et al. (2007), but adopting recent prescriptions for the dependence of M_{WR} on metallicity and a mass range $14.8-45 M_\odot$ for the total mass of binary systems. In particular, we consider the results of Georgy et al. (2009) which give the variation of M_{WR} as a function of the metallicity for all the core collapse SNe. In Tables 2 and 3 we show the $M_{WR} - Z$ relations extrapolated from the results of Georgy et al. (2009) and adapted to the metallicity range of our galactic models for SNIb/c and only Ic progenitors, respectively. In particular, in column 1 we show the relation between the minimum WR mass and metallicity for a range of Z values, indicated in the second column. Finally, in the third column we show the minimum WR mass corresponding to specific metallicities.

2.1 The computation of the supernova Ib/c rate

The distinguished features of Type Ib and Ic SNe is the lack of conspicuous hydrogen spectral lines. The SNe Ib/c

$M_{WR} - Z$ relation	Z range	$M_{WR}(M_{\odot})$
$M_{WR} = -15290Z + 113.76$	$Z \leq 0.004$	$\sim 52.6M_{\odot} @ Z = 0.004$
$M_{WR} = -5650Z + 75.20$	$0.004 < Z \leq 0.008$	$\sim 30M_{\odot} @ Z = 0.008$
$M_{WR} = -416.5Z + 33.33$	$0.008 < Z < 0.02$	$\sim 27.7M_{\odot} @ Z = 0.0134$
$M_{WR} = -230Z + 29.6$	$0.02 \leq Z \leq 0.04$	$\sim 25M_{\odot} @ Z = 0.020$
$M_{WR} = 20M_{\odot}$	$Z > 0.04$	$\sim 20.4M_{\odot} @ Z = 0.040$

Table 2. Relations between the minimal WR mass able to form SNeIb/c and metallicity, in different ranges of metallicity.

$M_{WR} - Z$ relation	Z range	$M_{WR}(M_{\odot})$
$M_{WR} = -10759Z + 116$	$Z \leq 0.008$	$\sim 30M_{\odot} @ Z = 0.008$
$M_{WR} = 750Z + 24$	$0.008 < Z < 0.02$	$\sim 34M_{\odot} @ Z = 0.0134$
$M_{WR} = -700Z + 53$	$0.02 \leq Z \leq 0.04$	$\sim 39M_{\odot} @ Z = 0.02$
$M_{WR} = 25M_{\odot}$	$Z > 0.04$	$\sim 25M_{\odot} @ Z = 0.04$

Table 3. Relations between the minimal WR mass able to form SNeIc and metallicity, in different ranges of metallicity.

occur preferentially in the vicinity of star forming regions and their progenitors are thought to be massive stars that have lost most of their H-rich (and perhaps their He-rich) envelopes via strong winds or transfer to a binary companion via Roche overflow. Approximately 25% of all Core Collapse SNe fall in the SNe Ib and SNe Ic category (Hamuy 2003).

The SN Ib/c and SNeIc rates have been calculated assuming both single WRs and stars in close binary systems as progenitors. In general:

$$\begin{aligned}
 SNR &= \int_{M_{WR}}^{100} \psi(t - \tau_M) \phi(M) dM + \\
 &+ F \int_{14.8}^{45} \psi(t - \tau_M) \phi(M) dM \\
 &\sim \psi(t) \left(\int_{M_{WR}}^{100} \phi(M) dM + F \int_{14.8}^{45} \phi(M) dM \right) \quad (5)
 \end{aligned}$$

where the lifetime τ_M of massive stars is considered negligible, $\psi(t)$ is the star formation rate and $\phi(M)$ is the IMF. The same equation is used for both SNe Ib/c and SNe Ic alone, and the only difference is in the minimum stellar mass of the progenitors, M_{WR} , varying as shown in Table 2 for the SNe Ib/c and in Table 3 for the sole SNe Ic. Concerning Type Ib/c SNe, in one case the evolution of M_{WR} , shown in Figure 3, is taken into account, while in the other case M_{WR} is assumed to be independent from metallicity and to be $25M_{\odot}$. Since, in this last case, the evolution of the SNR is quite the same for both the SN Types, we do not show the evolution of SNe Ic with M_{WR} constant. The factor F represents the fraction of massive binary stars producing Type Ib/c SNe. For the moment, this parameter is chosen to be equal to 0.15, (Calura & Matteucci, 2006). This value is motivated by the facts that first, in any galaxy, half of the massive stars are possibly in binary systems, and second, the fraction of massive stars in close binary system is

$\sim 30\%$, i.e. similar to the close binary frequency predicted for low mass systems (Jeffries & Maxted, 2005). Therefore, the estimated value for this parameter is given by:

$$F \sim 0.5 \cdot 0.3 \sim 0.15.$$

This is in good agreement with Podsiadlowski et al. (1992) who calculated that 15-30% of all massive stars (with initial masses above $8M_{\odot}$) could conceivably transfer mass to an interacting companion and end up as helium stars. However, we have tested also other values of the F parameter: in particular, for spirals we run models with F in the range 0.01-0.5 and found that the error on the predicted present time SN Ib/c rate is $\sim 0.003 \text{ SNe } yr^{-1}$, while for irregulars we run models with F in the range 0.01-0.3 (the value of 0.5 gives too high present time SN Ib/c rates relative to observations) with an error on the theoretical SN Ib/c rate of $\sim 0.0003 \text{ SNe } yr^{-1}$. We can safely conclude that in both cases F values lower than 0.15 are not enough to reproduce the observed Type Ib/c SN rates (see next paragraph), whereas higher but not unreasonable values (up to F=0.5), do not produce sensible differences in the results. Therefore, we do not exclude that our chosen value of F could be a lower limit.

3 RESULTS

Before comparing model results with the observed properties of galaxies, here we summarize some observational facts which are used to constrain our models:

- (i) the total fractional mass of gas in irregulars is:

$$(M_{\text{gas}}/M_{\text{tot}})_{t \sim 13 \text{ Gyr}} = [0.2 - 0.8]$$

whereas in spirals is:

$$(M_{\text{gas}}/M_{\text{tot}})_{t \sim 13 \text{ Gyr}} < 0.3$$

- (ii) the global average metallicity in irregulars is:

$$Z(t \sim 13 \text{ Gyr}) = [0.03 - 0.5] Z_{\odot}$$

whereas the average metallicity in the disk of a Milky Way like spiral is:

$$Z(t \sim 13 \text{ Gyr}) = [2 - 2.5] Z_{\odot},$$

where $Z_{\odot} \sim 0.0134$ (Asplund et al. 2009).

- (iii) The stellar mass vs. metallicity relation is an important observational constraint both for spirals and irregulars. In particular, these latter seem to be the lower part of the relation for spirals. The mass-metallicity relation indicates that the stellar mass of star forming galaxies is correlated with the galaxy metallicity: galaxies with larger stellar masses tend to have higher metallicities (Tremonti et al. 2004, Savaglio et al. 2005; Erb et al. 2006; Kewley & Ellison 2008; Maiolino et al. 2008).
- (iv) The predicted SN Ib/c rate (SNR Ib/c) should reproduce the following observational rates provided by Li et al. (2011):

$$SNR_{Ib/c} = 0.103_{-0.067}^{+0.136} SNuM \text{ (Irregulars)}$$

$$SNR_{Ib/c} = 0.113_{-0.025}^{+0.031} SNuM \text{ (Spirals)}$$

where $SNuM = SNe(100 \text{ yr})^{-1} (10^{10} M_{\odot})^{-1}$ is the SN Ib/c rate per unit mass, in good agreement with previous works

	Model Irr	Model Sp
Z	0.0096	0.03
$(M_{\text{gas}}/M_{\text{tot}})_{t \sim 13 \text{ Gyr}}$	0.66	0.017
$M_{\text{star}} [M_{\odot}]$	$1.4 \cdot 10^9$	$4.27 \cdot 10^{10}$
$12 + \log(O/H)$	8.6	9.12
$SFR [M_{\odot} \text{ yr}^{-1}]$	0.16	1.67

Table 4. Predictions of the Model Irr and Model Sp at present time: the total metallicity, total fractional mass of gas in the galaxy, stellar mass, oxygen abundance and star formation rate.

(i.e. Mannucci et al. (2005)). These observed rates can therefore be computed for galaxies of the same stellar mass as in our models and compared with our predicted rates.

The predicted values at present time of the total metallicity (Z), total fractional mass of gas in the galaxy ($M_{\text{gas}}/M_{\text{tot}}$), stellar mass in solar units (M_{star}) and oxygen abundance (expressed as $\log(O/H) + 12$) are showed in the table 4, respectively. It should be noted that the values of Z and $12 + \log(O/H)$ for the spiral galaxy are larger than solar, the reason is that they represent the average metallicities over the entire galactic disk, where the inner regions have oversolar values and the external ones have lower values.

We see that present models provides values in agreement with observations for the present total mass fraction of gas and for the average metallicity in both types of galaxies considered here.

In Figure 1, the time evolution of the star formation rates (expressed in M_{\odot}/yr) is plotted for the three different types of galaxies (Elliptical, Spiral and Irregular). The SFR increases until the energy injected into the ISM by stellar winds and SN(Ia, Ib, and II) explosions triggers a galactic wind. At that time, the thermal energy is equivalent to the binding energy of gas, and the gas is lost at a rate proportional to the SFR (eq.3) with a consequent drop of the SFR. Moreover, we can see that the present models well fit the present time averaged SFR both in spirals and in irregulars.

Figure 2 shows the predicted and observed mass-metallicity relation at the present time relative to small mass galaxies. In particular, we show both the best fit of Maiolino et al. (2008) of the data provided by Kewley & Ellison (2008) concerning star forming galaxies and the data and best fit of dwarf irregulars, as inferred by Lee et al. (2006). As one can see, our models lie close to the best fits. In our galaxy models the mass-metallicity relation arises naturally by adopting a smaller SFE in smaller galaxies. The above comparisons show that our chemical models very well reproduce many observed properties of the present day spirals and irregulars. Since, these present day properties results from the whole previous evolution, these good correspondence give some confidence that these models can be used to explore the much less well known early phases of these galaxies, which will hopefully be observed in greater details in a near future thanks to more powerful observational devices as the James Webb telescope and the ELT.

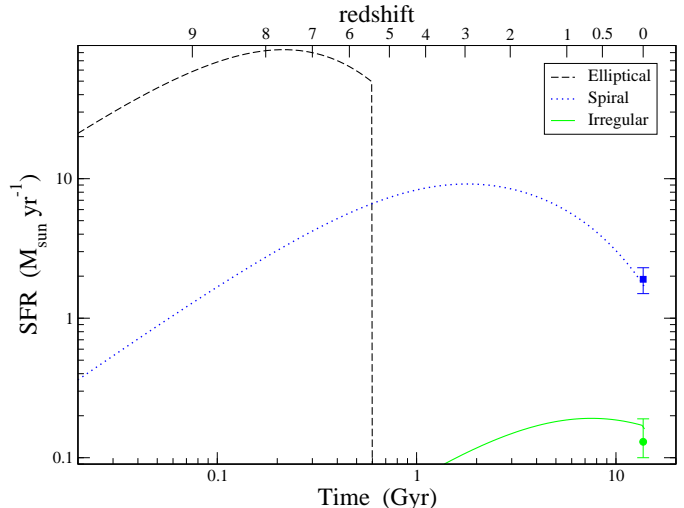


Figure 1. Predicted star formation rates of a typical elliptical, spiral and irregular galaxy, expressed in M_{\odot}/yr as functions of time and redshift; the redshift of galaxy formation is $z_f = 10$ in a Λ CDM cosmology. The infall masses for each type of galaxies are: $10^{11} M_{\odot}$ (elliptical, dashed line) $5 \cdot 10^{10} M_{\odot}$ (Spiral, dotted line) and $5 \cdot 10^9 M_{\odot}$ (Irregular, solid line). In the figure are shown also some average values for the present time SFR in spirals (square, Chomiuk & Povich, 2011) and in irregulars (circle, Harris & Zaritsky, 2009).

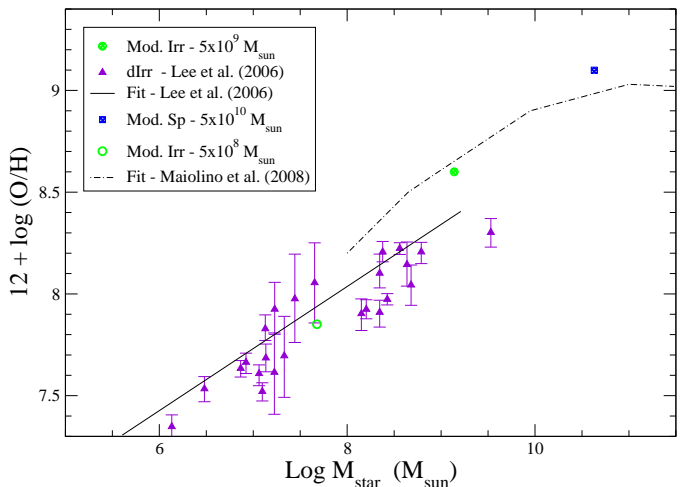


Figure 2. Predicted and observed mass-metallicity relation for irregular galaxies; the continuous curve represents the best fit to the data of Maiolino et al. (2008) relative to star forming galaxies together with data and fit obtained by Lee et al. (2006) for a sample of local dwarf galaxies (purple triangles). The points are the predictions for Model Irr (green circles) and Model Sp (blue square). Note that for the irregulars we are showing also a model with infall mass $M_{\text{infall}} = 5 \cdot 10^8$ and SFE=0.02 (open green circle).

In Figure 3 we show the evolution of the metallicity Z for our galaxies and the corresponding evolution of the minimum WR mass, according to the relations of Table 2 and 3. As one can see, owing to the milder increase of metallicity in the irregular galaxy, the M_{WR} varies more gradually as a function of time in this galaxy than in the spiral one. On

the other hand, the variation of M_{WR} in an elliptical is very fast in the very early phases.

In Figure 4, the SN Ib/c, Ic rates are shown as a function of time for Model Irr and Model Sp. Different rates arising under different assumptions concerning the SNIb/c and SNIc progenitors and their dependence on the initial stellar metallicity (see sect. 2.1). The percentage of SNe from binary systems represents $\sim 30\%$ of the total predicted rate. The points in Figure 4 are the observed SN Ib/c rates for an irregular (circle) and a spiral (square) galaxy provided by Li et al. (2011).

It is worth noting that the samples of SN-host galaxies usually include (due to an observational bias) small numbers of irregulars and there is no way to get out of this as long as the SN surveys will not include a large number of such irregular galaxies. Following Li et al.(2011), one can conservatively assume that the true value of the SN rate in Irregulars is between Li et al. (2011) and Mannucci et al (2005) estimates. In Figure 4 this uncertainty is included in the size of the error bars.

As one can see, the predicted present time rate of SNe Ib/c are consistent, within the error bars, with the observed ones.

An interesting quantity, often shown in literature, is the ratio between the SN Ib/c and the SN II rate, N_{Ibc}/N_{II} (i.e. Prantzos & Boissier 2003; Boissier & Prantzos 2009; Prieto et al. 2008; Smartt et al. 2009 and Smith et al. 2011). In order to have a more consistent comparison with the data we have plotted the N_{Ibc}/N_{II} and N_{Ic}/N_{II} ratios as functions of metallicity (see Figure 5). It is worth noting that when using N_{Ibc}/N_{II} and N_{Ic}/N_{II} vs metallicity, we cannot specify the galaxy type because the relation between mass and metallicity and the IMF are the same for all galaxy types. As one can see from Figure 5, our predictions are in good agreement with the data both in the case of SNe Ib/c (solid line) and SNe Ic (dashed line) and with previous calculations (Boissier & Prantzos, 2009).

4 THE LOCAL GRB/SNI_{BC} RATIO

Figure 4 shows the existence of a good match between the “expected” SNIb/c “local” rate, computed for spirals and irregulars, and the “observed” SN rates derived by Li et al. (2011). This agreement assesses quantitatively the reliability of the prescriptions that have been used in Sections 2 and 3 to derive the SNIb/c rate as a function of time and provides more weight to the results that will be presented in Section 5. When the metallicity effect on the minimum WR mass is taken into account, there is a difference only for irregulars, mainly at early times, due to the slower growth of metallicity in these systems.

It is interesting to compute the ratio of Type Ib/c SNe to GRBs (in the local Universe) and to do that we should compare the theoretical SNIb/c rates, shown in Figure 4, with the local rate of GRBs at the present time (triangle). The “canonical” value for the latter quantity ranges between ~ 0.5 GRB Gpc⁻³yr⁻¹ (Schmidt 2001) to ~ 1 event Gpc⁻³yr⁻¹ (Guetta et al. 2005). In order to compare the SNIb/c and the GRB rate in the right units we use the local GRB rate of 1.1 event Gpc⁻³yr⁻¹ (Guetta et al. 2005) taking into account the local density of B lu-

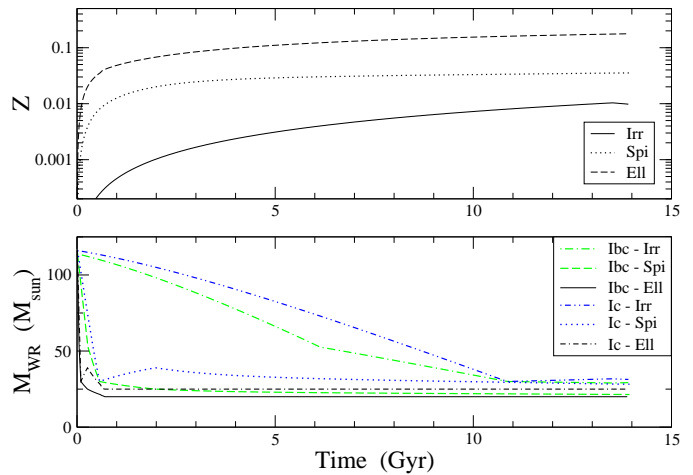


Figure 3. Upper panel: evolution of the total metallicity as a function of time for the Model Irr (solid line), Model Sp (dotted line) and for a typical elliptical (dashed line). Lower panel: evolution of the minimal mass of WR progenitors as a function of time for SNIb/c and SNIc in the Model Irr (green dotted-dashed line and blue double dotted-dashed line), Model Sp (green dashed line and blue dotted line) and for a typical elliptical (black solid line and black double dashed-dotted line).

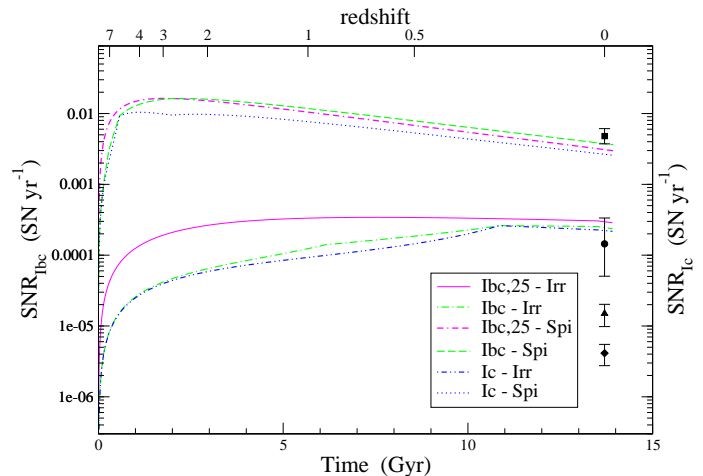


Figure 4. Supernova Ib/c and Ic rates as a function of time and redshift for Model Irr (magenta solid line, green dotted-dashed line and blue double dotted-dashed line) and Model Sp (dotted-double dashed magenta line, green dashed line and blue dotted line). The redshift of galaxy formation is $z_f = 10$ in a Λ CDM cosmology. The various model predictions for each rate depend on the different assumptions concerning the SNIb/c and SNIc progenitors and their dependence on the initial stellar metallicity: $M_{WR} = 25M_{\odot}$ (solid line for Model Irr and dotted-double dashed line for Model Sp), $M_{WR} = M(Z)$ (dashed line for SNIb/c and dotted line for SNIc in Model Sp; dashed-dotted line for SNIb/c and double dotted-dashed line for SNIc in Model Irr). The points are the observed SN Ib/c rates, obtained by multiplying the observed rate per unit mass (Li et al. 2011) by the present time stellar mass of the galaxy in Mod. Irr (circle) and Mod. Sp (square). In the Figure is shown also the local GRB rate provided by Guetta et al.(2005), triangle, and Salvaterra et al. (2011), diamond.

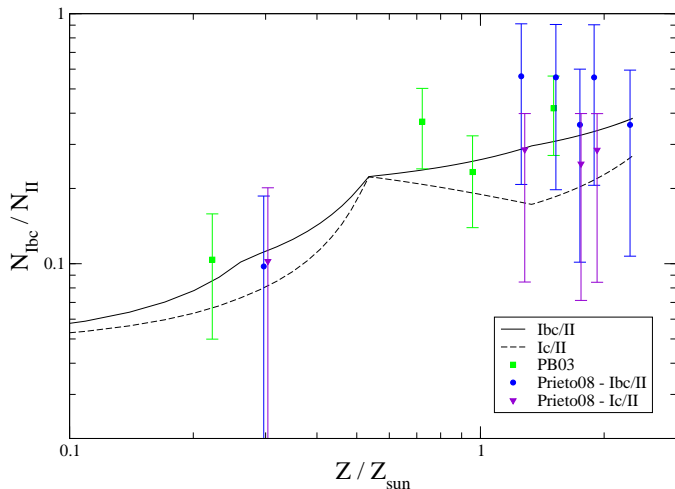


Figure 5. Number ratio of SNIb/c and Ic to SNI as a function of metallicity of the host galaxy (solid and dashed lines respectively). The circles and the triangles down are the values obtained by Prieto et al. (2008) from directly measured central metallicities for SNIbc and SNIc respectively while the squares are the results from Prantzos & Boissier (2003) using absolute magnitudes as a proxy to host metallicities.

minosity, $\sim 1.2 \cdot 10^8 L_{B,\odot} \text{ Mpc}^{-3}$ (e.g. Madau, Della Valle & Panagia 1998) and the B luminosity of the Milky Way, $2.3 \cdot 10^{10} L_{B,\odot}$. This approach gives $R_{GRB} \sim 2.1 \cdot 10^{-7} \text{ yr}^{-1}$. This “observed” rate has to be re-scaled by using the beaming factor, f_b^{-1} . The beaming factor accounts for the fact that a GRB does not light up the full celestial sphere but rather a fraction. There are several estimates of this parameter, $f_b^{-1} \leq 10$ (Guetta & Della Valle, 2007) for local and low luminosity GRBs, corresponding to $\theta > 25^\circ$, and $f_b^{-1} \sim 75 - 500$ (Guetta et al. 2005, Yonetoku et al. 2005; van Putten & Regimbau 2003, Frail et al. 2001), for high-luminosity GRBs, corresponding to beaming angles of $\sim 10^{-4}$.

If we conservatively assume, for “local” GRBs, $f_b^{-1} \leq 75$, we derive a “local” ratio GRB/SNIb/c of $\leq 3 \cdot 10^{-3}$ and $\leq 2 \cdot 10^{-2}$ in spirals and irregulars, respectively. This is an expected result, since not all SNe Ib/c will end up as long GRBs.

In Figure 4 we have shown the GRB rate provided by Guetta et al. (2005) in unit of yr^{-1} and re-scaled using the beaming factor $f_b^{-1} = 75 \pm 25$.

5 THE COSMIC SNI_{BC} AND GRB RATES

The cosmic SN and GRB rates are defined in an unitary comoving volume of the Universe. This definition is necessary to study the rates at high redshift where the morphology of the observed galaxies is not known. The cosmic rates refer, in fact, to a mixture of galaxies which can be different at every redshift. Both the cosmic Type Ib/c and GRB rates depend upon the SFR in galaxies but also on the galaxy and GRB luminosity functions. If these functions do not evolve with redshift then both the SN and GRB rates will trace the CSFR. On the contrary, the observed behaviour can be due to the evolution of the luminosity functions of galaxies (e.g.

number density evolution). The CSFR has now been measured up to very high redshift ($z \sim 8$), especially thanks to galaxies hosting GRBs (see Kistler et al. 2009). In Figure 6, we show a revised version of the CSFR predicted by Calura & Matteucci (2003) and obtained by taking into account the evolution of galaxies of different morphological type (ellipticals, spirals and irregulars), as described in the previous sections. In particular, the CSFR has been computed by assuming a pure luminosity evolution of galaxies, in other words, the main parameters of the Schechter (1976) galaxy luminosity function have been kept constant with redshift. To compute the CSFR we have adopted the following relation:

$$CSFR = \sum_k \psi_k(t) \cdot n_k^* [M_\odot \text{ yr}^{-1} \text{ Mpc}^{-3}], \quad (6)$$

where k identifies a particular galaxy type (elliptical, spiral, irregular) and $\psi_k(t)$ represents the history of star formation in each galaxy, as shown in Figure 1. The quantity n_k^* is the galaxy number density, expressed in units of Mpc^{-3} for each morphological galaxy type and it has been assumed to be constant and equal to the present time one, as derived by Marzke et al. (1994). This CSFR is therefore obtained by assuming that all galaxies started forming stars at the same time and that there is no number density evolution; these are very simple assumptions but they can be useful to disentangle the effect of the SFR from that of the luminosity function and to compare these results with predictions from hierarchical galaxy formation models. This predicted CSFR shows a high peak of star formation at very high redshift due to the contribution of the ellipticals which have formed their stars very early. This predicted high redshift CSFR is probably too high and unrealistic since the number density of ellipticals at high redshift could have been overestimated. In other words, the hypothesis of no number density evolution could be incorrect. On the other hand, the predicted CSFR for redshift $z < 6$ seems underestimated relative to the data. This does not mean that our galactic SF histories are wrong but again it could be due to neglecting the number density evolution of galaxies. We have adopted also CSFRs computed in the framework of the hierarchical clustering galaxy formation scenario, as well as the fit to the observed CSFR. In fact, in Figure 6 is also shown the CSFR obtained by Cole et al. (2001) best fitting the data collected by Hopkins (2004) from 1995 onwards. This same parametric form has been used later on by many authors such as Hopkins & Beacom (2006) and Blanc & Greggio (2008), since it fits also more recent data up to redshift $z=6$.

It is worth noting that also all the other theoretical CSFRs shown in Figure 6 are underestimating the CSFR at intermediate and low redshifts. To derive observationally the CSFR one should adopt some of the well known tracers of SF, in particular H_α , H_β , UV continuum. In these wavebands the effect of dust cannot be neglected and therefore the dust correction is necessary to obtain the correct CSFR. The differences between corrected and uncorrected data are generally large, as shown by Strolger et al. (2004). In particular, uncorrected data tend to show a strong decline of the CSFR for $z > 2$, whereas the corrected data show an almost constant CSFR for $z > 3$. Another important effect in the derivation of the CSFR is related to the uncertainty in the faint end of the luminosity function of galaxies.

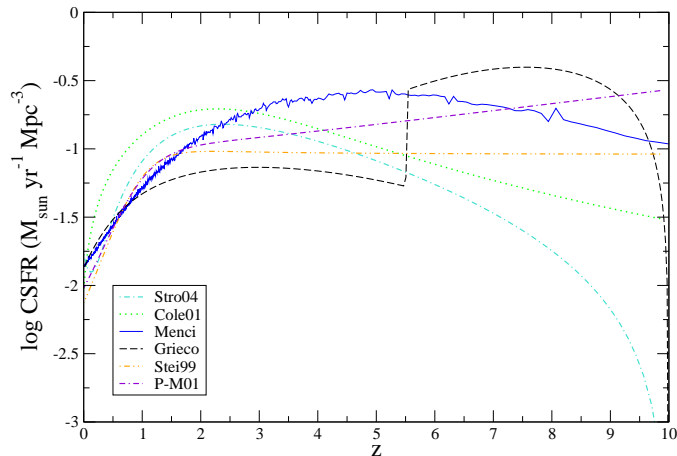


Figure 6. Evolution of different cosmic star formation rates with redshift: Menci, private communication (blue solid line), our model (black long-dashed line), Stroger 2004 (turquoise dashed-dotted line), Steidel 1999 (orange double dotted-dashed line), Porciani & Madau 2001 (violet double dashed-dotted line). The green dotted line is the fit (Cole et al. 2001) of the data collected by Hopkins (2004): this fit has then been extended up to redshift $z=6$.

By means of these different CSFRs we have then computed the cosmic SN Ib/c rate shown in Figures 7 where it is reported also the observed cosmic GRB rate. The adopted progenitors for SNe Ib/c are assumed to be single WR stars with constant minimum mass of $25M_{\odot}$ plus binary systems, as described in section 2.1. As one can see, the theoretical error in the CSFR increases towards high and very high redshift and it is roughly a factor of ten at $z=6$. Clearly at these high redshifts ($z > 6$) the uncertainties are still too large to draw any conclusion. In Figure 8 we show the predicted cosmic Type Ib/c SN rate obtained by adopting the Cole et al. (2001) CSFR and M_{WR} depending on Z , all the other assumptions being the same. Here we have considered the cosmic evolution of Z , and in particular we assumed the Z vs. time evolution typical of an elliptical galaxy of $10^{11}M_{\odot}$ as shown in Figure 3; this is because by weighting the Z vs. time of each galaxy on their number density, the Z vs. time relation of the ellipticals dominates at all redshifts. In fact, spheroids are very likely to be the responsible for the production of the bulk of metals in the Universe (see Calura & Matteucci 2004). As one can see in Figure 8, the effect of metallicity on the Type Ib/c SN progenitors is stronger at early times and produces a lower cosmic Type Ib/c SN rate. This effect would be similar if applied to all the CSFRs of Figure 6

Coming back to Figure 7, a visual inspection of this figure confirms that GRBs originating from the explosion of massive stars are only a tiny fraction of SNe Ib/c class. In particular, the comparison of the SN Ib/c rates with the Matsubayashi et al. (2005) semi-empirical track, suggests the ratio GRB/SN Ib/c to be $\sim 10^{-4}$ in the local Universe and to increase up to $\sim 10^{-3} - 10^{-2}$ all over the redshift range $z=1 \div 8$. Interestingly enough, the GRB/SNe Ib/c ratio at $z \sim 0$ nicely reproduces the “observed” ratio between the local GRB rate and the SN Ib/c rates obtained by other authors: $\sim 1GRB Gpc^{-3} yr^{-1}$ (Guetta et al. 2005)

and $\sim 2 \cdot 10^4 SN Ib/c Gpc^{-3} yr^{-1}$ (Guetta & Della Valle 2007), respectively. After taking these figures at their face values, we conclude that “local” and “low luminosity” GRBs ($L \leq 10^{49} ergs^{-1}$) barely need the correction for beaming and therefore we can infer that they emit almost isotropically. This result is in good agreement with observations (admittedly on scanty statistic). For example, for GRB 060218 Soderberg et al. (2006) find $\theta > 70deg$, for GRB 031203, $\theta > 30deg$ (Malesani, private communication) and $\theta > 25deg$ (corresponding to $f_b^{-1} \leq 10$) for “low luminosity” GRBs population (Guetta & Della Valle, 2007). The increasing ratio GRB/SN Ib/c $\sim 10^{-3} - 10^{-2}$ for $z \sim 1$, in the case of the Matsubayashi et al. (2005) GRB rate, may suggest either a different behavior for “cosmological” GRBs due to the existence of a different GRB population (e.g. Bromberg et al. 2011 and references therein) characterized by a larger beaming factor, likely of the order of $f_b^{-1} \sim 20 - 200$ (corresponding to a jet opening angle of $\sim 20deg-6deg$) or the Matsubayashi et al. semi-empirical track is still affected by the obvious bias which favors the discovery at high- z of only highly beamed GRBs. Similar conclusions (short of a constant) can be obtained by comparing the SN Ib/c rate track with the GRB track by Wanderman & Piran (2010) and with that by Salvaterra et al. (2011). In particular, the Salvaterra et al. (2011) rate is derived from a redshift complete sample of bright *Swift* GRBs under the assumption that GRBs did not experience luminosity evolution with redshift. It is worth noting that on the basis of the current studies, it is not possible to distinguish between a pure density and a pure luminosity evolution. In general, there is no agreement among different authors on this issue. Butler et al. (2010) suggest that pure density evolution models produce the observed number of GRBs at high- z , but in other works the luminosity evolution is used to explain the GRB rate (i.e. see Salvaterra et al. 2009b, Petrosian et al. 2009) increasing faster than some CSFR, such as that of Hopkins & Beacom (2006). This is because the Hopkins & Beacom (2006) CSFR is decreasing at high z . However, this behaviour of the CSFR needs to be confirmed by more data and at the moment we cannot exclude the CSFR to be flat at high z .

6 CONCLUSIONS

In this paper we have computed the Type Ib/c SN rates expected at the present time in irregular and spiral galaxies of different masses with the aim of predicting the variation with redshift of the SN Ib/c rate based on successful models for the chemical evolution of irregulars and spirals. We considered both single WR stars and massive stars in binary systems as SN Ib/c progenitors. We used stellar evolution results indicating that the minimum mass of WR stars is a function of the stellar metallicity thus suggesting a higher rate of SNe Ib/c in more metal rich galaxies. Then we considered various CSFRs as functions of cosmic time, both theoretically and observationally derived, and computed the cosmic Type Ib/c SN rates expected from the assumptions on Type Ib/c SN progenitors. These cosmic Type Ib/c SN rates were then compared to the observationally derived cosmic GRB rate. Our main conclusions can be summarized as follows:

- by taking into account WR progenitors depending on

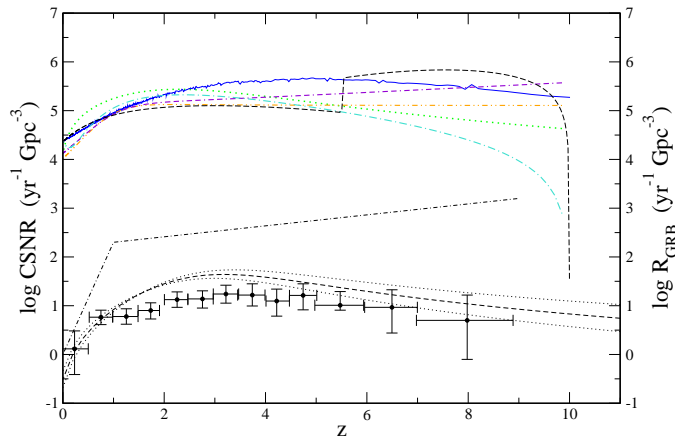


Figure 7. Comparison between the cosmic predicted Type Ib/c SN rates computed by means of all the CSFRs of Figure 6 and the number of observed GRBs at different redshift provided by Wanderman & Piran (2010), *Swift* data, (black circles with error bars) and Matsubayashi et al. (2005) (black dashed-dotted line in the lower part of the Figure). The short-dashed and the double dotted black line, below the Matsubayashi et al. (2005) rate, represent the best fit and the upper and lower limit, respectively, of the cosmic GRB rate obtained by Salvaterra et al. (2011). The CSNRs Ib/c are computed by means of CSFRs shown in Figure 6 and are indicated with the same symbols.

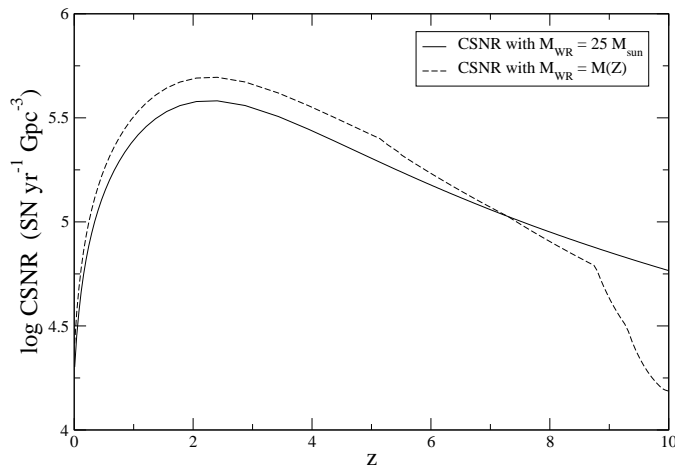


Figure 8. Comparison between the cosmic predicted Type Ib/c SN rates computed by means of the CSFR of Cole et al. (2001) and the different assumptions on M_{WR} : solid line refers to a constant M_{WR} whereas dotted line refers to the case of $M_{WR} = M(Z)$.

the metallicity and a fraction of massive close binary systems equal to 15% of all massive stars as SN Ib/c progenitors, it is possible to reproduce the present observed Type Ib/c SN rate both in dwarf metal poor irregular and in spiral galaxies. It is worth noting that the galactic evolution models adopted here are well reproducing the main chemical properties of these galaxies.

- If a dependence on stellar metallicity is assumed for the WR stars, differences arise in the Type Ib/c SN rates only at early evolutionary times in galaxies. Negligible differences are produced on the predicted local rates.

- We have compared the local observed Type Ib/c rates in spirals and irregulars with the local GRB rate and derived a local ratio GRB/SNe Ib/c of $\sim 3 \cdot 10^{-3}$. As expected, only a fraction of these SNe gives rise to GRBs.

- We took various CSFR histories and computed the cosmic Type Ib/c SN rates. Also in this case we considered both a constant minimum WR mass and a mass varying with metallicity. The effect of the dependence of M_{WR} on the metallicity is to predict lower cosmic Type Ib/c SN rates at very high redshift. We have then compared the cosmic Type Ib/c SN rates with the cosmic GRB rate derived from *Swift* data and found that the ratio GRB/SNe Ib/c $\sim 10^{-4}$. This confirms previous results that only a small fraction of all SNe Ib/c gives rise to GRBs, but our factor is smaller than what found in Bissaldi et al. (2007). The reason for this resides in the fact that we have adopted the recent GRB cosmic rate derived from *Swift* data, whereas in Bissaldi et al. (2007) the cosmic GRB rate was derived on the basis of semi-empirical estimates (Matsubayashi et al. 2005). On the other hand, if we compare our cosmic SN rates with the Matsubayashi et al. (2005) rate we confirm the results of Bissaldi et al. (2007), indicating a ratio GRB/SNIb/c rates of $\sim 10^{-3} - 10^{-2}$.

- Studies of GRBs and their hosts have revealed to be extremely important to trace galaxy evolution at very high redshifts, although the interpretation of cosmic diagrams is difficult since it involves assumptions on the luminosity function of both galaxies and GRBs. It is interesting to note that Salvaterra & Chincarini (2007) pointed out that by adopting the CSFR derived by Cole et al. (2001) and assuming a GRB luminosity function independent of redshift, one largely underestimates the number of high redshift GRBs detected by *Swift*. This fact could be interpreted in two ways: either the characteristic luminosity of GRBs increases with redshift or the CSFR at very high redshift is higher than in Cole et al. (2001). We have shown that a high CSFR can be achieved by means of monolithic like models of ellipticals producing stars at a very high rate and at very high redshift. However, no firm conclusions can be drawn on the CSFR at very high redshift because of the large uncertainties due to dust corrections.

ACKNOWLEDGMENTS

V.G. thanks Anahí Granada, Cyril Georgy and Luca Vinciolletto for many useful discussions.

REFERENCES

- Asplund M., Grevesse N., Sauval A. J. & Scott P., 2009, *ARA&A*, 47, 481
 Baron E., 1992, *MNRAS*, 255, 267
 Berger E., Penprase B.E., Cenko S.B., Kulkarni S.R., Fox D.B., Steidel C.C. & Reddy N.A., 2006, *ApJ*, 642, 979
 Bissaldi E., Calura F., Matteucci F., Longo F. & Barbiellini G., 2007, *A&A*, 471, 585
 Blanc G. & Greggio L., 2008, *Nature*, 13, 606
 Boissier S. & Prantzos N., 1999, *MNRAS*, 307, 857
 Boissier S. & Prantzos N., 2009, *A&A*, 503, 137

- Bradamante F., Matteucci F. & D'Ercole A., 1998, *A&A*, 337, 338
- Bromberg O., Nakar E. & Piran T., 2011, arXiv:1107.1346
- Butler N.R., Bloom J.S. & Poznanski D., 2010, *ApJ*, 711, 495
- Calura F. & Matteucci F., 2003, *ApJ*, 596, 734
- Calura F., Matteucci F. & Menci N., 2004, *MNRAS*, 353, 500
- Calura F. & Matteucci F., 2006, *ApJ*, 652, 889
- Calura F., Pipino A., Chiappini C., Matteucci F. & Maiolino R., 2009, *A&A*, 504, 373
- Campisi M.A., Tapparello C., Salvaterra R., Mannucci F., & Colpi M., 2011, arXiv:1105.1378
- Chiappini C., Matteucci F. & Gratton R., 1997, *ApJ*, 477, 765
- Chiappini C., Matteucci F. & Romano D., 2001, *ApJ*, 554, 1044
- Chomiuk L. & Povich M.S., 2011, *AJ*, 142, 197
- Cole S. et al., 2001, *MNRAS*, 326, 255
- Conselice C.J. et al., 2005, *ApJ*, 633, 29
- Erb D.K., Shapley A.E., Pettini M., Steidel C.C., Reddy N.A., Adelberger K.L., 2006, *ApJ*, 644, 813
- Fynbo J.P.U. et al., 2003, *A&A*, 406, L63
- Fynbo J.P.U. et al., 2006, *A&A*, 451, L47
- Frail D.A. et al., 2001, *ApJ*, 562, L55
- Fruchter A.S. et al., 2006, *Nature*, 441, 463
- Fukugita M., Hogan C.J. & Peebles P.J.E., 1998, *ApJ*, 503, 518
- Georgy C., Meynet G., Walder R., Folini D. & Maeder A., 2009, *A&A*, 502, 611
- Gorosabel J. et al., 2005, *A&A*, 444, 711
- Guetta D., Piran T. & Waxman E., 2005, *ApJ*, 619, 412
- Guetta D., & Della Valle M., 2007, *ApJ*, 657, L73
- Hamuy M., 2003, arXiv:astro-ph/0301006v1
- Harris J. & Zaritsky D., 2009, *AJ*, 138, 1243
- Hjorth J. & Bloom J.S., 2011, arXiv:1104.2274
- Hopkins, X., 2004, *ApJ*, 615, 209
- Hopkins A.M. & Beacom J.F., 2006, *ApJ*, 651, 142
- Iwamoto K., Mazzali P.A., Nomoto K. et al., 1998, *Nature*, 395, 672
- Iwamoto K., Brachwitz F., Nomoto K., Kishimoto N., Umeda H., Hix W.R. & Thielemann Friedrich-K., 1999, *ApJS*, 125, 439
- Jeffries R.D. & Maxted P.F.L., 2005, *AN*, 326, 944
- Kewley L.J. & Ellison S.L., 2008, *ApJ*, 681, 1183
- Kistler M. D., Yüksel H., Beacom J. F., Hopkins A. M. & Wyithe J. S. B., 2009, *ApJ*, 705, L104
- Kobulnicky H.A. & Fryer C.L., 2007, *ApJ*, 670, 747
- Krühler T. et al., 2011, arXiv:1108.0674
- Lanfranchi G.A. & Matteucci F., 2003, *MNRAS*, 345, 71
- Lee H., Skillman E.D., Cannon J.M., Jackson D.C., Gehrz R.D., Polomski E.F. & Woodward C.E., 2006, *ApJ*, 647, 970
- Li L.-X., 2008, *MNRAS*, 388, 1487
- Li W., Chornock R., Leaman J. et al., 2011, *MNRAS*, 412, 1473
- Lin L., Liang E. & Zhang S., 2010, *Science in China G: Physics and Astronomy*, 53, 64
- MacFadyen A. & Woosley S., 1999, *ApJ*, 524, 262
- Maiolino R. et al., 2008, *A&A*, 488, 463
- Mannucci F., Della Valle M., Panagia N. et al., 2005, *A&A*, 433, 807
- Mannucci F., Salvaterra R. & Campisi M.A., 2011, *MNRAS*, 414, 1263
- Martin C.L., 1999, *ApJ*, 513, 156
- Martin C.L., Kobulnicky H.A. & Heckman T.M., 2002, *ApJ*, 574, 663
- Marzke R.O., Geller M.J., Huchra J.P. & Corwin H.G., Jr., 1994, *AJ*, 108, 437
- Matteucci F. & Francois P., 1989, *MNRAS*, 239, 885
- Matteucci F., 2001, *Nature*, 414, 253
- Modjaz M. et al., 2008, *AJ*, 135, 1136
- Paczynski B., 1998, *ApJ*, 494, L45
- Petrosian V., Bouvier A. & Ryde F., 2009, arXiv:0909.5051
- Pipino A. & Matteucci F., 2004, *MNRAS*, 347, 968
- Prantzos N. & Boissier S., 2003, *A&A*, 406, 259
- Prieto J.L., Stanek K.Z. & Beacom J.F., 2008, *ApJ*, 673, 999
- Prochaska J.X. et al., 2004, *ApJ*, 611, 200
- Salvaterra R. & Chincarini G., 2007, *ApJ*, 656, L49
- Salvaterra R., Guidorzi C., Campana S., Chincarini G. & Tagliaferri G., 2009b, *MNRAS*, 396, 299
- Salvaterra R. et al., 2011, *ApJ*, submitted, arXiv:1112.1700
- Savaglio S. et al., 2005, *ApJ*, 635, 260
- Savaglio S., 2006, *New Journal of Physics*, 8, 195
- Savaglio S., Glazebrook K. & Le Borgne D., 2009, *ApJ*, 691, 182
- Schmidt X., 2001, *ApJ*, 552, 36
- Smartt S.J., 2009, *ARA&A*, 47, 63
- Smith N., Li W., Filippenko A.V. & Chornock R., 2011, *MNRAS*, 412, 1522
- Soderberg A.M. et al., 2004, *ApJ*, 606, 994
- Soderberg A.M. et al., 2006, *Nature*, 442, 1014
- Spitoni E., Matteucci F., Recchi S., Cescutti G. & Pipino A., 2009, *A&A*, 531, 72
- Stanek K.Z. et al., 2006, *AcA*, 56, 333S
- Strolger L.G., Riess A.G., Dahlen T. et al., 2004, *ApJ*, 613, 200
- Tanvir N.R. & Levan A.J., 2007, arXiv:0709.0861
- Tanvir N.R. et al., 2009, *Nature*, 461, 1254
- Tremonti C.A. et al., 2004, *ApJ*, 613, 898
- van den Hoek L.B. & Groenewegen M.A.T., 1997, *A&AS*, 123, 305V
- van Putten M.H.P.M. & Regimbau T., 2003, *ApJ*, 593, L15
- Wainwright C., Berger E. & Penprase B.E., 2007, *ApJ*, 657, 367
- Wanderman D. & Piran T., 2010, *MNRAS*, 406, 1944
- Wolf C. & Podsiadlowski P., 2007, *MNRAS*, 375, 1049
- Woosley S.E., 1993, *ApJ*, 405, 273
- Woosley S.E. & Weaver T.A., 1995, *ApJS*, 101, 181
- Woosley S.E. & Bloom J.S., 2006, *ARA&A*, 44, 507
- Yin J., Magrini L., Matteucci F., Lanfranchi G.A., Gonçalves D.R. & Costa R.D.D., 2010, *A&A*, 520, A55
- Yonetoku D., Yamazaki R., Nakamura T., & Murakami T., 2005, *MNRAS*, 362, 1114
- Yoon S.-C., Woosley S.E. & Langer N., 2010, *ApJ*, 725, 940
- Zhang B., Woosley S.E. & MacFadyen A.I., 2003, *ApJ*, 586, 356